

Design of a solar system with a PID controller based on the Tyrannosaurus optimization algorithm

Kadhim Sabah Rahimah^{1,2,3}, Issa Ahmed Abed⁴, Afrah Abood Abdul Kadhim¹

¹Department of Electrical Engineering Technology, Basrah Engineering Technical College, Southern Technical University, Basra, Iraq

²Department of Computer Engineering Technology, Shatt Al-Arab University College, Basra, Iraq

³Ministry of oil-south Refineries Company, Basra, Iraq

⁴Department of Control and Automation Engineering Technology, Basrah Engineering Technical College, Southern Technical University, Basra, Iraq

Article Info

Article history:

Received Dec 7, 2024

Revised Feb 3, 2026

Accepted Feb 17, 2026

Keywords:

Converter

Maximum power point tracking
Optimization

Proportional integral derivative
Solar

ABSTRACT

Although photovoltaic (PV) power generation systems are an efficient way to use solar energy, their conversion efficiency is very low. Keeping the DC output power from the panel consistent is the key challenge with solar PV systems. Radiation and temperature are two variables that can impact a panel's output power. This study proposes a unique hunting-based optimization technique called the Tyrannosaurus optimization algorithm (TROA). It is demonstrated that the TROA can be used to achieve maximum power point tracking (MPPT) for lithium-ion battery charging with solar panels. Tyrannosaurus Rex hunting techniques served as the model for this approach. MPPT is used to regulate the solar array's output in PV systems. A buck converter is used by the charge controller to convert DC to DC. To provide the most power, it is utilized to balance the impedance of batteries and solar panels. To maximize power transfer, the algorithm modifies the gating signal's duty cycle based on the voltage and current detected by the solar panel. Three well-known optimization methods are contrasted with TROA's performance: gorilla troops optimization (GTO) algorithm, particle swarm optimization (PSO), and cultural algorithm (CA). In contrast to current approaches, the proposed approach has yielded superior results.

This is an open access article under the [CC BY-SA](https://creativecommons.org/licenses/by-sa/4.0/) license.



Corresponding Author:

Issa Ahmed Abed

Department of Control and Automation Engineering Technology

Basrah Engineering Technical College, Southern Technical University

Basra, Iraq

Email: issaahmedabed@stu.edu.iq

1. INTRODUCTION

The predominance for solar technology worldwide in the future is a result of its striking qualities and ongoing quest for new sources of energy. To meet its present needs, every country has started to progressively construct photovoltaic (PV) plants [1], [2]. Because of their enormous power needs, developing nations like India will need to depend on sustainable energy sources like wind and solar power. Arctic icebergs melt as a result of climate change brought on by rising global temperatures. As a result, every nation began looking for alternate methods to reduce pollution [3]. There are very few obstacles in the way of the grid's integration and conversion [4]. When one system is converted to another, such as when DC to DC or DC to AC is converted, the conversion process usually occurs. The most significant conversion system among them is DC to DC [5]-[7]. Lead acid batteries are still popular but experiments with lithium-ion batteries are also underway; the key aspect here is price. A stand-alone PV system uses solar energy. Solar

energy is transformed into electrical energy by PV panels. Nonlinear internal characteristics are seen in PV systems. A solar PV system's voltage and power characteristics are influenced by temperature and radiation. To monitor maximum output power, maximum power point tracking (MPPT) is necessary since solar panels are expensive batteries that are interfaced with a DC-to-DC converter. The major reasons why lead acid batteries are utilized are their extended service life, low self-discharge, broad working temperature range, and lack of maintenance requirements. When compared to the PV panel, the battery installation costs are lower. However, owing to its short service life, the battery has a higher lifetime cost than a PV system. Longer periods of low PV energy availability or incorrect charging and discharging shorten battery life. The charging process needs to be controlled in order to get a high state of charge (SOC) and increase battery life. To extend the life of batteries, they must be properly charged. In a freestanding PV system, the battery charging controller is principally in charge of halting reverse current flow, preventing deep discharge when the system is under load, and fully charging the battery without going overboard. The battery model, PV model, and battery charging system with buck converter are all included in this proposed system. A buck converter, which is also used for battery charging, controls the flow of electricity from the PV panel to the battery and load. The PV panel's power must be measured using an MPPT control algorithm. The Tyrannosaurus optimization algorithm (TROA) is used in MPP tracking.

The complete system is modeled using MATLAB/Simulink, and the outcomes are displayed. The battery charging current monitoring technique used in this work is depicted in Figure 1. To increase the solar panel's maximum power production, MPPT systems are utilized. Despite changes in load factors, temperature, and irradiance, the solar PV panel's output remains constant. In order for solar panels to generate electricity more effectively, buck converters are used to convert DC to DC electricity [8]. In standalone PV systems, buck converters are utilized for DC-DC step-down and battery storage [9]. Diodes, thyristors, power metal-oxide-semiconductor field-effect transistors (MOSFETs), and other components are frequently used in exchange applications. By operating the DC-DC converter in a closed loop and altering the MOSFETs' gate signal, the output voltage is limited [10]. For monitoring solar output from PV panels, a variety of MPPT algorithms are available. For battery charging applications, step-down converters provide greater efficiency. TROA is a flexible and efficient method for solving temperature and isolation issues. Insolation, short for incident or incoming solar radiation, is a method that measures the total quantity of solar radiation energy received by a region over a given time period. The measurement of radiation is in watts per square meter or W/m².

The amount of radiation that is reflected or absorbed in PV systems depends on an object's reflectivity. The amount of insolation that enters a surface is largest when it faces the Sun directly. As the angle between the direction of the sun's beams at a right angle to the surface and that direction rises, the insolation falls according to the cosine of the angle [9]. The buck converter uses buck operation, which steps down the voltage and is useful for charging batteries and low-power applications. The purpose of this study was to employ the MPPT and TROA to improve the efficiency of battery charging with solar energy. Simulink was utilized to assess the inquiry's efficacy.

The system description that the MPPT block is mostly concerned with is shown in Figure 1 of the current work. Using a recently developed optimization technique called TROA, the proportional integral derivative (PID) controller's gain settings are adjusted to optimize the power output from the model PV. The pulse width modulation (PWM) technique is utilized to supply the chopper's gate with the proper pulses.

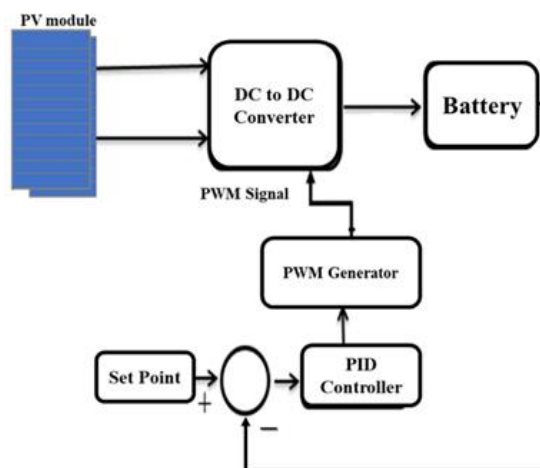


Figure 1. The planned PV power system's block diagram

2. RESEARCH METHOD

2.1. Buck converter DC-DC

A conversion of bucks in essence, DC-DC consists of power switches that control pulses, like bipolar junction transistors (BJTs) or MOSFETs. Figure 2 shows the circuit configuration, by lowering the high-level DC voltage to the low-level DC voltage, the MOSFET acts as a power switch. The output voltage of this circuit never rises above the input voltage [11]. This circuit's objective is to produce a complete DC output. The DC output voltage in the basic circuit was produced using an LC low-pass filter. The diode reverses biases and begins supplying energy to the load and inductor once the switch is activated. Once the switch is deactivated, the diode will conduct inductor current and become forward-biased. To power the load, some of its energy reserves will be used. This circuit design can be applied as a high-level voltage connection to a low load and as a high-range step-down converter [12]-[15]. The buck converter's primary parameters are shown in Table 1.

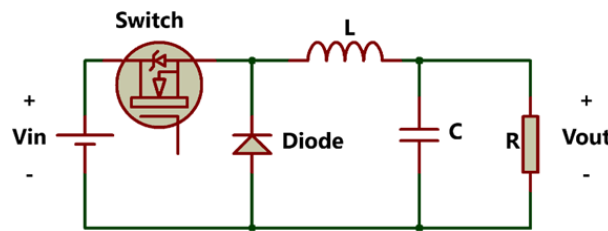


Figure 2. Buck converter topology

Table 1. The buck converter's primary parameters

Type		
Switching frequency	f_c	10 kHz
Load	Battery	12 V
Inductance	L	2.63e-4 H
Capacitance	C_1, C_2	33 μ F, 309 μ F

The connection between input voltage (V_S) and duty cycle causes a low output voltage related to buck converters. The output voltage's value (V_o), the duty cycle has an impact on. The (1) can be used to calculate the output voltage based on the duty cycle, D. When constructing the buck converter, the inductor value is determined using (2) and (3). To guarantee the circuit's continuous operation, the inductor's value, as determined by (2), must be 25% more than its minimum value, L_{min} . In addition, the maximum and minimum inductor currents (I_{max} and I_{min}) can be found using (4), (5), (7), and to maintain a constant current flow, the I_{min} value must be greater than zero, and the output ripple voltage, which can be expressed as a percentage of the output voltage, can be used to determine the value of the capacitor, C using (7).

$$D = \frac{V_o}{V_S} \quad (1)$$

$$L_{min} = \frac{D(1-D)}{2f} \quad (2)$$

$$L = 1.25L_{min} \quad (3)$$

$$I_L = \frac{V_o}{R} \quad (4)$$

$$I_{max} = I_L + \frac{\Delta i_L}{2} \quad (5)$$

$$I_{min} = I_L - \frac{\Delta i_L}{2} \quad (6)$$

$$C = \frac{(1-D)}{8L \left(\frac{\Delta V_o}{V_o}\right) f} \tag{7}$$

2.2. The maximum power point tracking algorithm utilizing proportional integral derivative

One type of feedback control loop technology is a PID controller that combines derivative, integrator, and proportional control. Typically, it constantly calculates the error value, $e(t)$. The error value is the discrepancy between the intended value and the processed output. PID controllers react fast, deliver the desired output as effectively as feasible, and avoid overshooting or process delays. As a result, automatic control is possible. Figure 3 displays the PID controller's block diagram. The control output will likewise be high if the error is high. The present error values are handled by the proportional gain K_p . The time-integrated past values of error are integrated using an integrator in the integral gain K_i . Because of this integral term, error is eliminated by the control output, which is reliant on the error's current cumulative error value. The derivative gain in a differentiator removes error by generating a control signal in reaction to a sudden change in current. It has a mathematical expression in (8).

$$u(t) = K_p e(t) + K_i \int_0^t e(t) dt + K_d \frac{d}{dt} e(t) \tag{8}$$

In the Laplace domain, its corresponding Laplace transform is expressed as in (9).

$$U(S) = K_p E(S) + \frac{K_i}{S} E(s) + K_d S E(S) \tag{9}$$

The proportional gain constant is denoted by K_p , the integral gain constant by K_i , the differential gain constant by K_d , the control variable by $u(t)$, and the error value by $e(t)$.

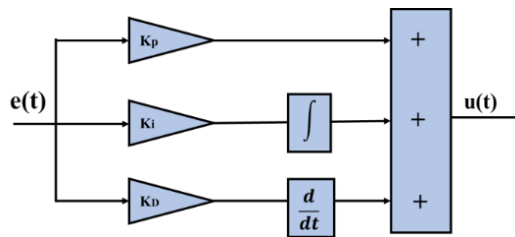


Figure 3. The PID controller's design

The DC load voltage reference value (V_{ref}). This extra input is used by the TROA-tuned MPPT controller to increase the duty cycle of the DC-DC boost converter for the best power point tracking. Figure 4 shows the architecture of the control.

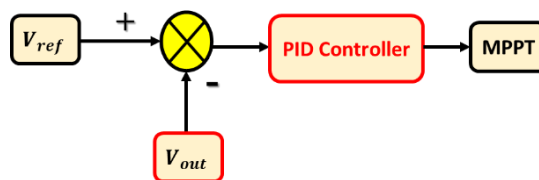


Figure 4. PID control

2.3. Maximum power point tracking algorithm

The junction of a PV module's I-V curve and the load line, or the load's I-V relationship, defines the module's operational point when it is directly connected to a load. A PV module's output is typically boosted to make up for its low power yield during the winter. This mismatch between a PV module and a load necessitates the use of a larger PV module, increasing the total cost of the system. A maximum power point tracker can assist alleviate this problem by maintaining the PV module's operating point at the MPP. MPPTs can catch over 97% of PV electricity when set correctly [16], [17]. The temperature and radiation at the

MPP's location in the I-V plane are always fluctuating. The MPPT controller's tracking algorithm is what makes it possible for it to locate the MPP. The voltage must then be raised to the proper level and maintained there using an MPPT controller. The MPPT's measurements of PV voltage and current should be followed by the PV operating voltage. The voltage is reduced to a level appropriate for battery charging by a synchronous buck mode DC-DC converter once it receives the module's output. To isolate the module from the battery, the MPPT algorithm modifies the PWM to the DC-DC converter to gradually alter the duty cycle. The PV module's operational parameter is suitably optimized in the current research employing the TROA.

2.4. Optimization algorithm

It is possible to define many real-world issues as optimization problems with several parameters that need to be addressed. Finding a solution or solutions to reduce or maximize the values of one or more objectives is the mathematical definition of optimization. Moreover, an optimization problem is referred to as restricted when it calls for certain parameters to satisfy one or more restrictions.

2.4.1. Tyrannosaurus optimization algorithm

a. Inspiration

These dinosaurs, and particularly the Tyrannosaurus Rex, were present in western North America around 66 million years ago. The Tyrannosaurus reigns supreme among the dinosaur species. In popular culture, the Tyrannosaurus Rex is referred to as T. rex or T-Rex, is one of the most well-known dinosaurs. Rex means "king" in Latin. Members of a genus, these massive theropod dinosaurs were 3.66 to 3.96 meters tall, 12.3 to 12.4 meters long, it typically weighed between 8.4 and 14 metric tons.

People assume that tyrannosaurus rex, like lions, wolves, and other animals, are apex predators since they are among the largest carnivores on Earth. The T-Rex was a scavenger, according to other researchers [10]. Many scientists now concur that the T. Rex was both an active hunter and a scavenger, despite the fact that it was once uncertain if it was an apex predator or a scavenger [18]. Among other dinosaurs of its kind, it is renowned for its hunting behavior due to its powerful biting force Figure 5.



Figure 5. Tyrannosaurus [19]

b. Suggested algorithm

This section starts by describing the inspiration behind the recommended strategy. Next, an algorithm and flowchart are presented with the mathematical model. The TROA simulates Tyrannosaurus rex hunting to update population positions. Prey selection, which finally selects the best option, hunting and pursuit, and population initiation are the three primary steps of the process [19]-[22]. Figure 6 displays a diagram that illustrates the TROA algorithm, and the algorithm describes the specific phases of this mechanism's procedure.

- Initialization
- Hunting
- Selection

Let us see the steps in detail:

i) Initialization

TROA begins by employing randomness to generate an initial population, where each prey's location correlates to an optimization problem solution, much like any other heuristic technique. The (10) can be used to express the stochastic totality.

$$X_i = \text{rand}(np, dim) * (ub - lb) + lb \quad (10)$$

Where X_i indicates the location of the i -th prey, $X_i=[X_1, X_2, \dots, X_n]$ within the upper and lower boundaries, X_i is created at random, with n being the dimension, where the population size is denoted by np , the upper and lower boundaries of the search space by ub and lb , respectively, and the search space's dimension by dim .

ii) Hunter and pursuing

As with wolves, lions, and other apex predators, a T-Rex pursues its victim. Upon spotting its closest target, the T-Rex attempts to hunt. Prey may attempt to flee or protect itself from predators on occasion. When T-Rex are young, they hunt at random because they are chasing and capturing prey.

$$X_{new} = \begin{cases} x_{new} & \text{if } rand() < Er \\ \text{Random else} & \end{cases} \quad (11)$$

Therefore, as (11) illustrates, when the T-Rex starts hunting, the prey starts to disintegrate, and the T-Rex tracks it by updating its location. Where Er is the estimated chance of reaching the scattered prey.

$$X_{new} = x + rand() * sr (tpos * tr - target * pr) \quad (12)$$

When the hunting success rate, denoted by sr , falls between $[0.1, 1]$; hunting is unsuccessful if sr is 0, and the position of the associated prey must be changed; the Tyrannosaurus rex's running speed, tr , is measured between $[0, 1]$, while the prey's running speed, pr , is recorded between $[0, 1]$ as well. The minimum distance the prey must go to avoid the rex is known as the target.

iii) Selection

The position of the prey—that is, the present and previous locations of the intended prey—is the basis for the selection process. If the prey runs away or protects itself from the predator, the prey position is zero, which prevents the T-Rex from hunting. The comparative fitness function, which is produced by comparing the fitness function, is displayed in (13) [19], [21].

$$x_i^{k+1} = \begin{cases} \text{update the target position if } f(x) < f(x_{new}) \\ \text{target is zero otherwise} & \end{cases} \quad (13)$$

A representation of the updated prey's fitness function by $f(X_{new})$, whereas the initial random prey position's fitness function is represented by $f(x)$. Tyrannosaurus Rex cannot hunt $f(x) < f(x_{new})$, as shown by (13), if the prey position becomes 0.

The suggested optimization procedure is organized according to the T-Rex's predatory behavior. Algorithm 1 describes the methodical steps of the Tyrannosaurus optimisation algorithm (TOA). The procedure starts with the random initialization of the prey's position and the assessment of its fitness based on the specified objective function. The algorithm then determines the position that is closest to the target, directing the T-Rex's hunting movement through a sequence of mathematical updates. The iterative cycle makes sure that the prey's position is refined by comparing fitness values, eventually arriving at the best solution.

Algorithm 1. T-Rex hunting optimization strategy for prey capture

Input: Population size, maximum iterations, and objective function $f(x)$.

Output: the optimal position of the target.

- 1- Begin
- 2- Using Equation (10), randomly initialize the prey's position.
- 3- Use Equation (10) to compute fitness.
- 4- Determine the prey's closest location and set the T-Rex to pursue it.
- 5- Use Equations (11) and (12) to begin the T-Rex hunting procedure.
- 6- Assess the suitability of the prey's new habitat.
- 7- Update the prey's position if the $f(x) < f(x_{new})$.
- 8- The goal equals zero if the condition fails.
- 9- stop

Pseudo code 1 summarizes the procedural logic of the TOA to make its computational implementation more understandable. In (10) is used to determine the prey's starting position. Its fitness is then assessed to choose the main target. The movement of the T-Rex is controlled by a stochastic parameter

E_r inside the iterative while-loop. In (11) is used to update the prey's location if the condition ($rand() < E_r$) is met; if not, a random update is carried out. After calculating the new fitness using (12), the system uses conditional logic to either reset the objective or update the target's location. Until the ideal value is discovered, and the termination requirements are satisfied, this cycle keeps going.

Pseudo code 1. T-Rex algorithm

```

First, use Equation (10) to determine the prey's position.
Determine the prey's minimum position and compute its fitness.
Look at the intended prey
The start of the while loop
Make the T-Rex move at random.
if rand() < Er
Use equation (11) to update the prey's position.
else
Randomly update the prey's location.
End the if
Use Equation (12) to determine the new fitness
If  $f(x) < f(x_{new})$ .
Update the target's and prey's locations.
else
The objective is zero.
Close the if
Search for the best value.
t = t + 1
Complete while
Go back

```

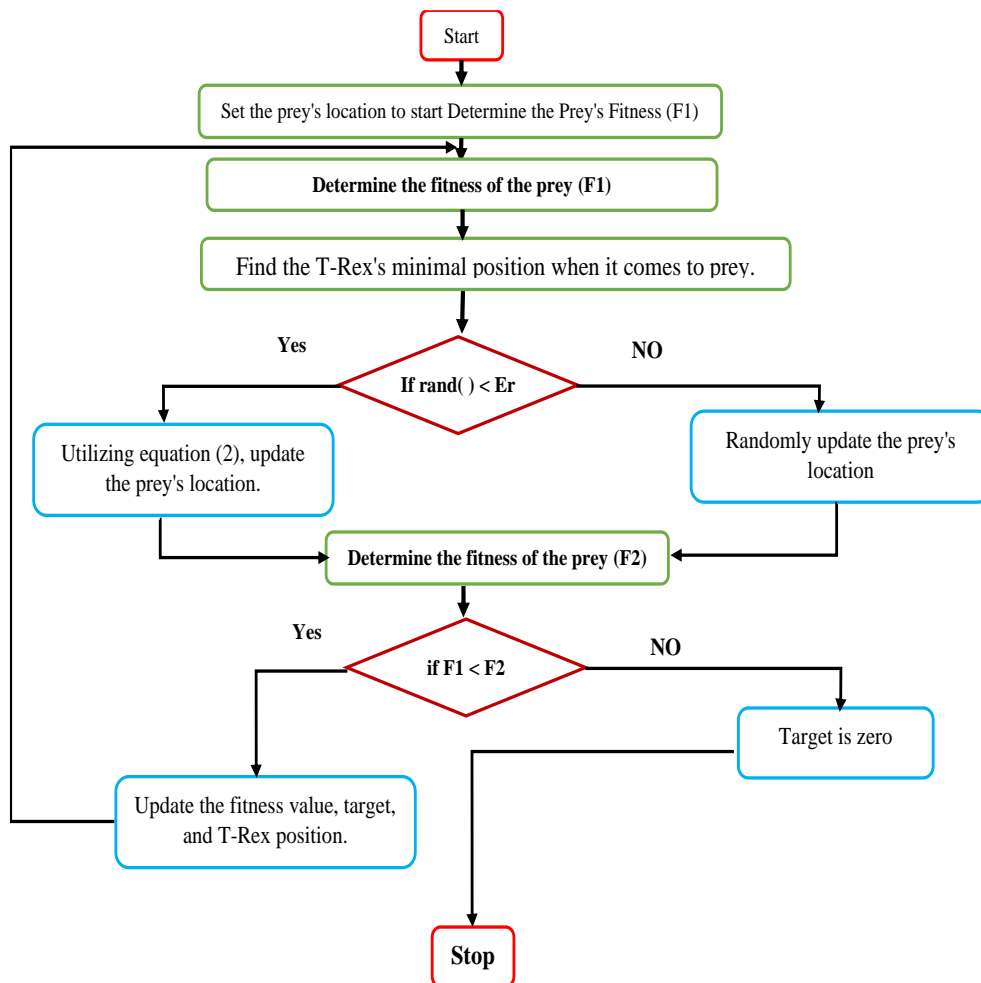


Figure 6. Diagram representing the TROA algorithm

2.5. The Tyrannosaurus optimization algorithm-based MPPT algorithm with variable step size

As seen, when the step size is fixed, the conventional MPPT algorithms perform admirably. However, the most problematic issues include the inability to adhere to the MPP point when atmospheric conditions change quickly, the delayed convergence, and oscillations around the MPP point. Tracking can be finished quickly by accounting for larger phases. Slower dynamics oscillations can be attenuated by using a smaller step size. Many contributions that took advantage of variable step size have made significant progress in solving these problems. With this method, the system uses the attributes of the PV array to automatically determine the step size. Depending on each operating situation, the step size must strike a satisfying balance between oscillations and dynamism. A novel variable step size MPPT algorithm with less oscillations, quicker response times, and easier comprehension is presented in this study [23]-[26]. Figure 7 displays the variable step MPPT that Simulink generated.

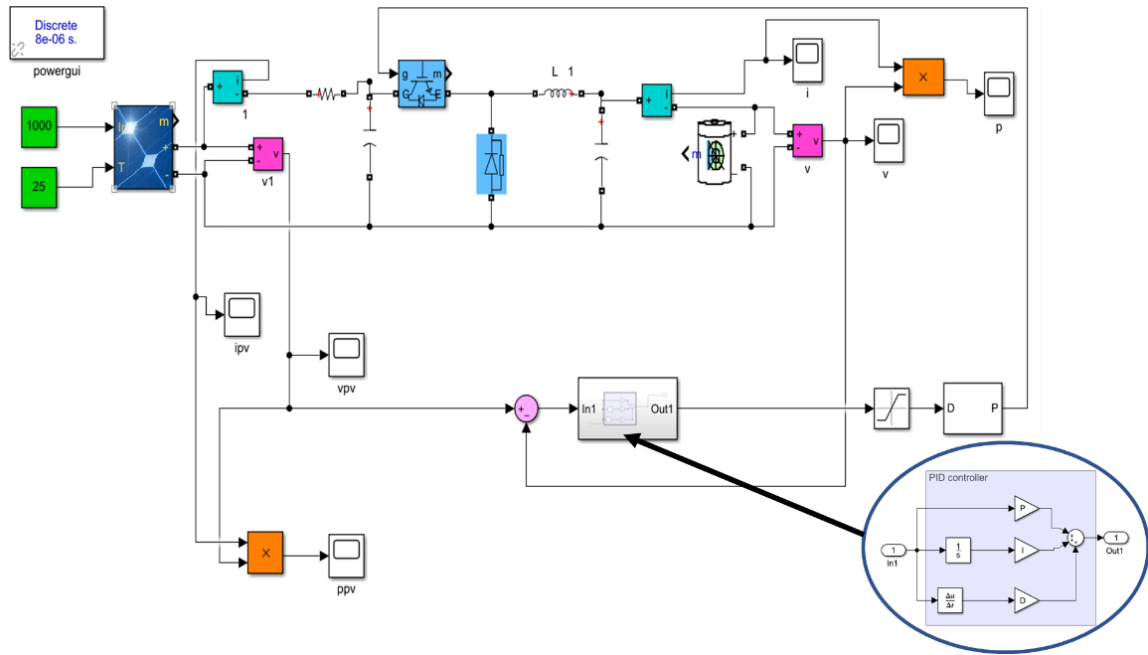


Figure 7. Implementation of MPPT variable step TROA MATLAB/Simulink

3. RESULTS AND DISCUSSION

We utilize the Solar PV mono-crystalline 315.016 W module from Znshine PV-Tech ZXP6-72-315-P to simulate and evaluate the suggested approach. Table 2 lists the Znshine PV-Tech PV module's technical specifications.

Table 2. Presents the technical parameters of the Znshine PV-Tech 315.016W PV module

Type	ZXP6-72-315-P	
The voltage in a circuit that is not plugged	V_{oc}	45.22 V
The current of a short circuit	I_{short}	8.95 A
Maximum voltage	V_{mpp}	37.28 V
Maximum current	I_{mpp}	8.45 A
Maximum power	P_m	315.016 W
It determines how many cells there are in a series	N_s	72
It determines how many cells there are in a parallel	N_p	1
Parallel resistance	R_p	252.2616 Ω
Series resistance	R_s	0.2702 Ω

A PV module model made with MATLAB/Simulink version R2019a, The PC has an Intel(R) Core (TM) i5-2410M CPU and 6 GB of RAM. Analyze the relationship between tracking the largest power point and employing artificial intelligence techniques to produce the maximum power. A comparative simulation analysis shows the efficacy of the proposed MPPT algorithms. By building the simulations under identical

meteorological conditions, the simulation investigations were finished in steady-state settings. The solar energy system is subjected to the application of particle swarm optimization (PSO), cultural algorithm (CA), gorilla troops optimization (GTO), and TROA. These algorithms were initially put to the test by varying each technique's settings and monitoring the system's reaction. The main emphasis is on how quickly the power ripple produced by The MPP is followed by steady-state oscillations surrounding it. The population size and dimension for all of the approaches used in this work were set at (10, 20, 30) and (50, 100,150). Testing was done on four algorithms: the first was the CA, which had the following values: $\alpha=0.3$, $\beta=5$, and acceptance ratio $\text{accept}=0.35$. The second was PSO, where the inertia weights were $w_{Max}=0.7$, $w_{Min}=0.4$, and $C_1 = C_2 = 1.49445$. In GTO, the third is $p=0.03$, $B_{eta}=3$, and $w=7$. In TROA, the fourth is $sr=0.7$, $tr=0.2$, and $pr=0.15$, respectively. The PID controller was evaluated with these methods in three different iterations and search agent conditions. The fitness function is determined by taking the absolute error by time (ITAE) performance index.

3.1. A comparison study of the Tyrannosaurus optimization algorithm

This section compares the suggested approach with three other optimization algorithms: PSO, cultural approach, and GTO. It is clear from Table 3 that TROA performed better in terms of exploration and exploitation when it came to solving the benchmark test issues than the other techniques. For a sample simulation run, the fitness value change as a function of iterations is shown by the convergence curve. The test result obtained for comparison with alternative algorithms and the recommended method is shown in Table 3. This suggests that TROA works more effectively than alternative algorithms. The convergence curves demonstrate that TROA typically advances in larger steps and hits near-optimal values in comparatively early repetitions. PSO, however, experiences slower convergences. On the other hand, TAOA was able to produce findings with greater precision through this search procedure as opposed to using the standard CA, GTO, and PSO. This phenomenon may be seen in the TROA curves, which indicate that most fitness functions can be achieved at relatively lower levels. TROA is hence more stable. It is evident from Figure 8 convergence curve comparison analysis, Figure 8(a) convergence curve illustration of the optimal values at iteration 50, Figure 8(b) convergence curve illustration of the optimal values at iteration 100, and Figure 8(c) convergence curve representation of best values at Iteration 150, that the TROA converges more quickly than other algorithms. On an arithmetic scale, the fitness value is represented by the y-axis. This logarithmic scale aids in determining how the fitness curve values of the various methods differ from one another.

When compared to alternative methods, the fitness value of the suggested algorithm varies significantly. The target prey's dynamic position-updating approach is to blame for this. Because the TROA covers the entire search space with fewer iterations than other methods, it performs better.

Table 3. Outcomes of TROA and other algorithms following 10 runs, (50, 100, 150) iterations, as well as population (10, 20, 30)

Response parameters	PSO			GTO			CA			TROA		
No. of iteration	50	100	150	50	100	150	50	100	150	50	100	150
k_p	10.57	11.03	150	146.27	20.29	29.80	15.43	15.08	15.15	11.85	9.91	30.77
k_i	250	250	129.46	248.30	233.29	233.64	250	250	250	67.55	33.69	90.01
k_d	20.31	19.27	7.18	10.03	18.59	32.84	13.87	13.99	14.00	28.86	28.55	72.36
Fitness function	0.056	0.0352	0.0352	0.0012	0.0017	0.0013	0.0011	0.0011	0.0011	1.91e-07	1.53e-07	7.82e-08
Settling time	9.36	9.06	8.74	8.55	9.06	10.13	9.06	9.09	9.06	4.29	4.48	4.29
	ms	ms	ms	ms	ms	ms	ms	ms	ms	ms	ms	ms
Overshoot	0.909	0.909	0.909	0.909	0.909	0.909	0.909	0.909	0.909	0.819	0.819	0.819
	0%	%	%	%	%	%	%	%	%	%	%	%
Rise time	19.72	19.70	19.62	19.46	18.91	19.99	19.52	19.52	19.53	1.76	1.87	1.76
	ms	ms	ms	ms	ms	ms	ms	ms	ms	ms	ms	ms
No. of search agent	10	20	30	10	20	30	10	20	30	10	20	30

Table 1 displays a PV panel's electrical properties. Figures 9 to 11 depict the PV module's performance, accordingly. A PV panel's power is displayed using the TROA-PID Control method in Figure 9. Figure 10 displays the voltages of a PV panel using TROA-PID control and a buck converter. To keep the

voltage and current constant, the TROA-PID controller adjusts the pulse width. The TROA-PID approach is used by a buck converter to supply a constant voltage and current to the load. Figures 12 and 13 show the voltage and load current, respectively. Figure 14 shows a buck converter's load power under TROA-PID control. The data makes it clear that TROA-based MPPT provides accurate tracking for both changeable and constant environmental conditions in the converters.

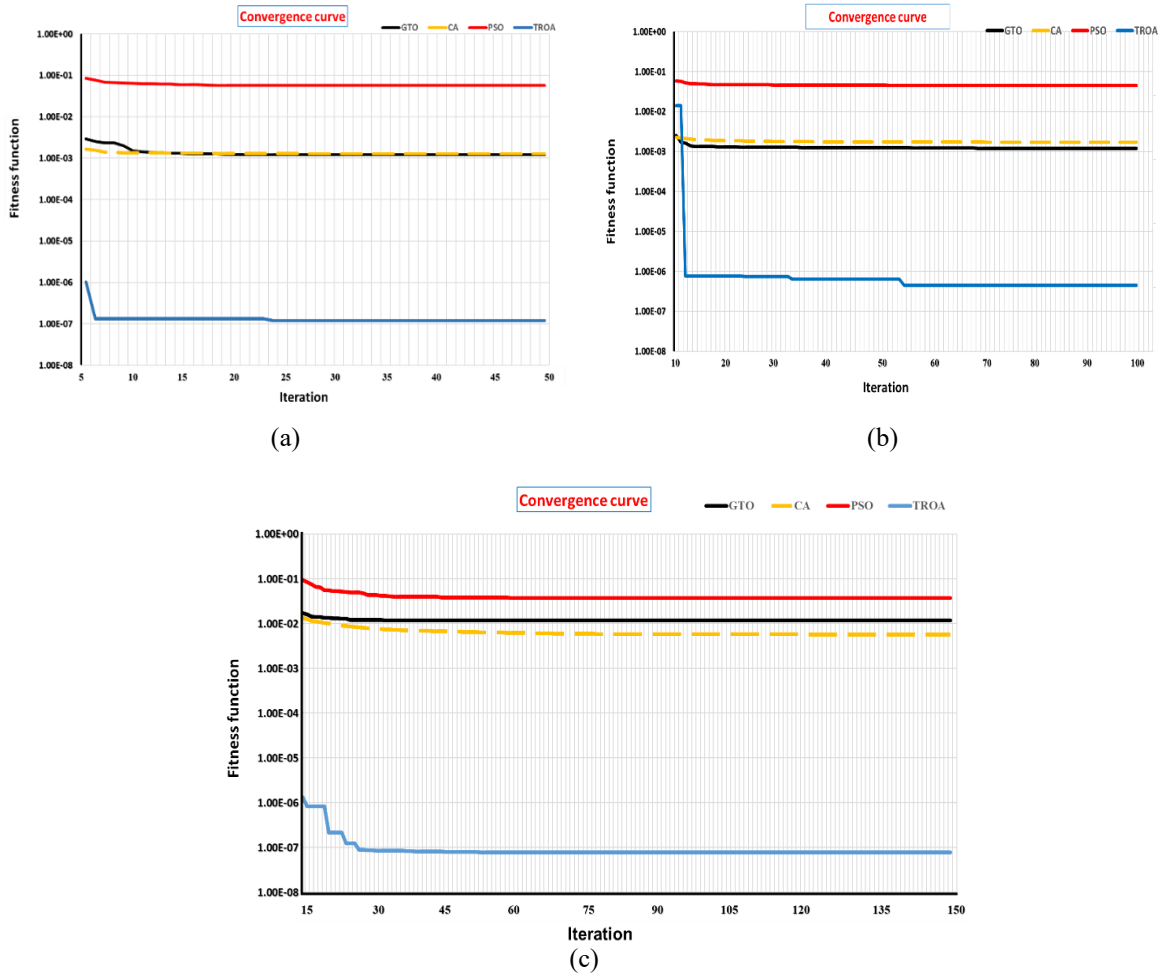


Figure 8. Convergence curve comparison analysis; (a) convergence curve illustration of the optimal values at iteration 50, (b) convergence curve illustration of the optimal values at iteration 100, and (c) convergence curve representation of best values at Iteration 150

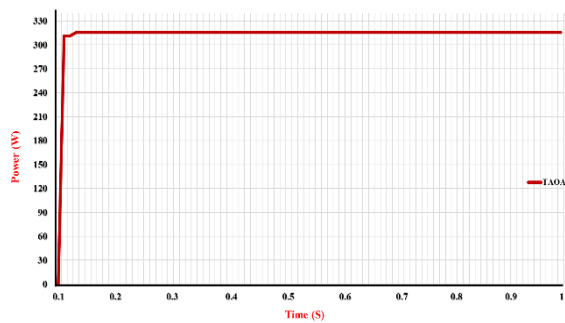


Figure 9. PV power using TROA-PID control MPPT

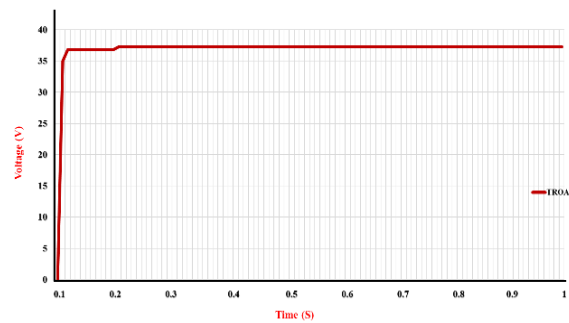


Figure 10. PV voltage using TROA-PID control MPPT

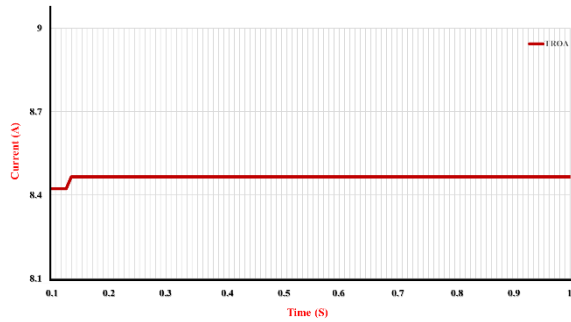


Figure 11. PV current using TROA-PID control MPPT

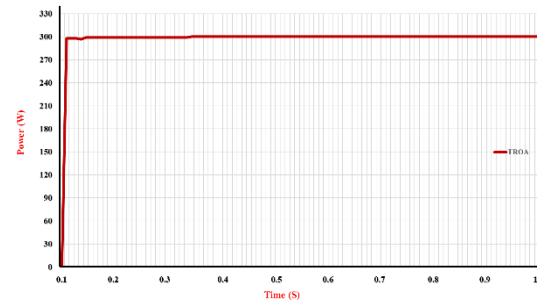


Figure 12. The load power of the buck converter

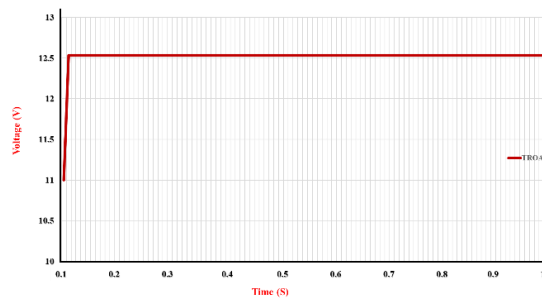


Figure 13. The load voltage of the buck converter

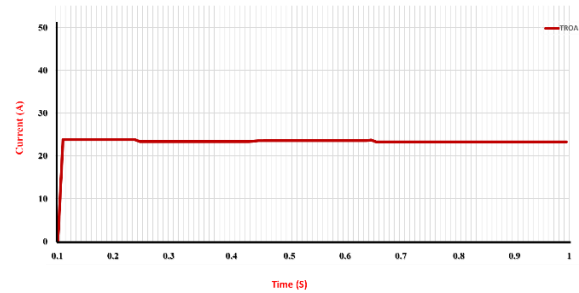


Figure 14. The load current of the buck converter

4. CONCLUSION

The study presents a novel meta-heuristic approach to optimization issues that is modeled on Tyrannosaurus Rex's hunting style. This approach uses two inputs: the prey's position and the T-Rex. The prey will attempt to flee at a specific speed as the T-Rex pursues it with a predetermined success rate. About academic performance indices, the MPPT method was refined and verified. The converter outputs corresponding to different controllers are obtained and tuned with the best results in the MPPT. It has been found that when scaling gains are applied at the proper values, the TROA - PID system generates the most useful outputs. The outcomes of the Tyrannosaurus algorithm outperform those of the other methods. It is possible to use the established MPPT technology for other application-based systems. The tuning process is simplified since TROA-PID does not require data gathering for offline system identification. Additionally, the tuning process is trustworthy and not under human control. Because of this, the TROA- PID can be recognized as an adaptive tuning technique that can be directly embedded into the actual PV-MPPT hardware of any configuration. The TROA outperforms other approaches since it uses fewer iterations to cover the entire search space. Over ten runs in all operational settings, the average fitness function value was $1.53e-07$. In contrast, the PSO, GTO, and CA for the other theories are 0.0352, 0.0017, and 0.0011, respectively. The approach will be expanded for multi-objective optimization situations in future studies. Future academics and researchers who study or do research on MPPT systems may find the results to their interest.

FUNDING INFORMATION

This work was partially supported by Southern Technical University under scientific research awards, No. 9/7934, 10 Sep. 2025.

AUTHOR CONTRIBUTIONS STATEMENT

This journal uses the Contributor Roles Taxonomy (CRediT) to recognize individual author contributions, reduce authorship disputes, and facilitate collaboration.

Name of Author	C	M	So	Va	Fo	I	R	D	O	E	Vi	Su	P	Fu
Kadhim Sabah Rahimah	✓	✓	✓	✓	✓	✓		✓	✓	✓				✓
Issa Ahmed Abed		✓				✓		✓	✓	✓	✓	✓		
Afrah Abood Abdul Kadhim	✓		✓	✓			✓			✓	✓		✓	✓

C : Conceptualization

M : Methodology

So : Software

Va : Validation

Fo : Formal analysis

I : Investigation

R : Resources

D : Data Curation

O : Writing - Original Draft

E : Writing - Review & Editing

Vi : Visualization

Su : Supervision

P : Project administration

Fu : Funding acquisition

CONFLICT OF INTEREST STATEMENT

Authors state no conflict of interest.

DATA AVAILABILITY

Upon reasonable request, the corresponding author [Issa Ahmed Abed] may disclose the data supporting the study's conclusions.

REFERENCES

- [1] M. H. Rashid, *Power electronics handbook*. Butterworth-heinemann, 2017.
- [2] H. R. Muhammad, "Power Electronics-Circuits, Devices, and Applications," *Up. Saddle River, NJ, Pearson Prentice Hall*, 2004.
- [3] H. C. Foong, M. T. Tan, Y. Zheng, and I. Ng, "Adaptive optimal controller based on genetic algorithm for digital DC-DC converters," in *2011 IEEE International Symposium on Industrial Electronics*, 2011, pp. 119–124, doi: 10.1109/ISIE.2011.5984143.
- [4] X. Wang, M. Wu, L. Ouyang, and Q. Tang, "The application of GA-PID control algorithm to DC-DC converter," in *Proceedings of the 29th Chinese Control Conference*, 2010, pp. 3492–3496.
- [5] S. Radhika and V. Margaret, "A review on dc-dc converters with photovoltaic system in dc micro grid," in *Journal of Physics: Conference Series*, 2021, vol. 1804, no. 1, p. 12155.
- [6] G. S. Rao, S. Raghu, and N. Rajasekaran, "Design of feedback controller for boost converter using optimization technique," *International Journal of Power Electronics and Drive Systems (IJPEDS)*, vol. 3, no. 1, pp. 117-128, 2013, doi: 10.11591/ijpeds.v3i1.1737.
- [7] M. R. Dave and K. C. Dave, "Analysis of boost converter using PI control algorithms," *International Journal of Engineering Trends and Technology*, vol. 3, no. 2, pp. 71–73, 2012.
- [8] J. T. Bialasiewicz, "Renewable energy systems with photovoltaic power generators: Operation and modeling," *IEEE Transactions on industrial Electronics*, vol. 55, no. 7, pp. 2752–2758, 2008, doi: 10.1109/TIE.2008.920583.
- [9] M. Kasper, D. Bortis, and J. W. Kolar, "Classification and comparative evaluation of PV panel-integrated DC-DC converter concepts," *IEEE Transactions on Power Electronics*, vol. 29, no. 5, pp. 2511–2526, 2013, doi: 10.1109/TPEL.2013.2273399.
- [10] K. I. Hwu and T. J. Peng, "A novel buck-boost converter combining KY and buck converters," *IEEE Transactions on Power Electronics*, vol. 27, no. 5, pp. 2236–2241, 2011, doi: 10.1109/TPEL.2011.2182208.
- [11] X. Zhang, T. Wang, H. Bao, Y. Hu, and B. Bao, "Stability effect of load converter on source converter in a cascaded buck converter," *IEEE Transactions on Power Electronics*, vol. 38, no. 1, pp. 604–618, 2022, doi: 10.1109/TPEL.2022.3199234.
- [12] A. S. Samosir, T. Sutikno, and L. Mardiyah, "Simple formula for designing the PID controller of a DC-DC buck converter," *International Journal of Power Electronics and Drive Systems (IJPEDS)*, vol. 14, no. 1, pp. 327-336, 2023, doi: 10.11591/ijpeds.v14.i1.pp327-336.
- [13] M. H. Taghvaei, M. A. M. Radzi, S. M. Moosavain, H. Hizam, and M. H. Marhaban, "A current and future study on non-isolated DC-DC converters for photovoltaic applications," *Renewable and Sustainable Energy Reviews*, vol. 17, pp. 216–227, 2013, doi: 10.1016/j.rser.2012.09.023.
- [14] M. S. Ali, S. K. Kamarudin, M. S. Masdar, and A. Mohamed, "An overview of power electronics applications in fuel cell systems: DC and AC converters," *The Scientific World Journal*, pp. 1-9, 2014, doi: 0.1155/2014/103709.
- [15] D. Izci, B. Hekimoğlu, and S. Ekinçi, "A new artificial ecosystem-based optimization integrated with Nelder-Mead method for PID controller design of buck converter," *Alexandria Engineering Journal*, vol. 61, no. 3, pp. 2030–2044, 2022, doi: 10.1016/j.aej.2021.07.037.
- [16] M. A. B. Siddique, A. Asad, R. M. Asif, A. U. Rehman, M. T. Sadiq, and I. Ullah, "Implementation of incremental conductance MPPT algorithm with integral regulator by using boost converter in grid-connected PV array," *IETE Journal of Research*, vol. 69, no. 6, pp. 3822–3835, 2023, doi: 10.1080/03772063.2021.1920481.
- [17] J. Ahmed, Z. Salam, M. Kermadi, H. N. Afrouzi, and R. H. Ashique, "A skipping adaptive P&O MPPT for fast and efficient tracking under partial shading in PV arrays," *International Transactions on Electrical Energy Systems*, vol. 31, no. 9, p. e13017, 2021, doi: 10.1002/2050-7038.13017.
- [18] W. Yang, C. Zhao, X. Tan, and X. Bian, "A Novel Near-infrared Spectral Variable Selection Approach Based on Discretized Tyrannosaurus Optimization Algorithm," *Chinese Journal of Analytical Chemistry*, p. 100703, 2026, doi: 10.1016/j.cjac.2026.100703.
- [19] V. S. D. M. Sahu, P. Samal, and C. K. Panigrahi, "Tyrannosaurus optimization algorithm: a new nature-inspired meta-heuristic algorithm for solving optimal control problems," *e-Prime-Advances in Electrical Engineering, Electronics and Energy*, vol. 5, pp.

- 1-21, 2023, doi: 10.1016/j.prime.2023.100243.
- [20] E. Güler and M. Z. Bilgin, "Forecasting Solar Energy Production Using Artificial Neural Networks and Tyrannosaurus Optimization Algorithm," *Sustainability*, vol. 18, no. 2, pp.1-29, 2026, doi: 10.3390/su18020690.
- [21] S. Zhang, H. Shi, B. Wang, C. Ma, and Q. Li, "A dynamic hierarchical improved tyrannosaurus optimization algorithm with hybrid topology structure," *Mathematics*, vol. 12, no. 10, pp. 1-33, 2024, doi: 10.3390/math12101459.
- [22] L. Zheng, X. Feng, M. Wu, and M. He, "Improved Tyrannosaurus Optimization Algorithm with Mixed Strategies," in *Proceedings of the 2024 3rd International Conference on Artificial Intelligence and Intelligent Information Processing*, 2024, pp. 99–104, doi: 10.1145/3707292.3707349.
- [23] M. Joisher, D. Singh, S. Taheri, D. R. Espinoza-Trejo, E. Pouresmaeil, and H. Taheri, "A hybrid evolutionary-based MPPT for photovoltaic systems under partial shading conditions," *IEEE Access*, vol. 8, pp. 38481–38492, 2020, doi: 10.1109/ACCESS.2020.2975742.
- [24] A. Loukriz, S. Messalti, and A. Harrag, "Design, simulation, and hardware implementation of novel optimum operating point tracker of PV system using adaptive step size," *The International Journal of Advanced Manufacturing Technology*, vol. 101, no. 5, pp. 1671–1680, 2019, doi: 10.1007/s00170-018-2977-7.
- [25] A. Harrag and S. Messalti, "PSO-based SMC variable step size P&O MPPT controller for PV systems under fast changing atmospheric conditions," *International Journal of Numerical Modelling: Electronic Networks, Devices and Fields*, vol. 32, no. 5, p. e2603, 2019, doi: 10.1002/jnm.2603.
- [26] J. Águila-León, C. Vargas-Salgado, D. Díaz-Bello, and C. Montagud-Montalvá, "Optimizing photovoltaic systems: A meta-optimization approach with GWO-Enhanced PSO algorithm for improving MPPT controllers," *Renewable Energy*, vol. 230, p. 120892, 2024, doi: 10.1016/j.renene.2024.120892.

BIOGRAPHIES OF AUTHORS



Kadhim Sabah Rahimah    obtained a diploma in Electronic Technologies in 2014 from the Technical Institute of Technology in Basra, Iraq's Southern Technical University. earned a bachelor's degree in electrical engineering from Southern Technical University in Iraq in 2014 and a master's degree in electrical engineering technologies in 2024. Artificial intelligence, solar energy, control systems, and high-pressure electric power generation are among his areas of interest. He currently teaches in Shatt Al-Arab University's Department of Computer Techniques Engineering and works as an engineer at South Refineries Company. He has participated in multiple international conferences, attended many national and worldwide conferences and workshops, and authored several scholarly articles in foreign magazines. He can be contacted at email: k.s.sabah@fgs.stu.edu.iq.



Issa Ahmed Abed    obtained his B.Sc. and M.Sc. in Control and Computing from the University of Basrah, Iraq's Department of Electrical Engineering in 2002 and 2005, respectively. In 2014, he received his Ph.D. in Control and Computing from University Tenaga Nasional in Malaysia. He is currently a professor at Engineering Technical College Basrah, Southern Technical University, Iraq, where he is the head of Department of Control and Automation Engineering Technology. Artificial intelligence, solar energy, robotics, control systems, and image processing are some of his areas of interest. He can be contacted at email: issaahmedabed@stu.edu.iq.



Afrah Abood Abdul Kadhim    obtained her B.Sc. and M.Sc. in power and machine from the University of Basrah, Iraq's Department of Electrical Engineering in 2002 and 2006, respectively. She currently teaches at Southern Technical University's Basrah Engineering Technical College in Iraq. Her interests include robotics, artificial intelligence, power, machines, and control. She can be contacted at email: afrah.alasady@stu.edu.iq.